

Reliability-based topology optimization of imperfect structures considering uncertainty of load position

*Original*

Reliability-based topology optimization of imperfect structures considering uncertainty of load position / Habashneh, M., Cucuzza, R., Aela, P., Movahedi Rad, M.. - In: STRUCTURES. - ISSN 2352-0124. - ELETTRONICO. - 69:(2024). [10.1016/j.istruc.2024.107533]

*Availability:*

This version is available at: 11583/2994035 since: 2024-10-31T13:50:39Z

*Publisher:*

Elsevier

*Published*

DOI:10.1016/j.istruc.2024.107533

*Terms of use:*

This article is made available under terms and conditions as specified in the corresponding bibliographic description in the repository

*Publisher copyright*

(Article begins on next page)



# Reliability-based topology optimization of imperfect structures considering uncertainty of load position

Muayad Habashneh<sup>a</sup>, Raffaele Cucuzza<sup>b</sup>, Peyman Aela<sup>c</sup>, Majid Movahedi Rad<sup>a,\*</sup>

<sup>a</sup> Department of Structural and Geotechnical Engineering, Széchenyi István University, H-9026 Győr, Hungary

<sup>b</sup> Department of Structural, Building and Geotechnical Engineering, Politecnico Di Torino, Corso Duca degli Abruzzi, 24 - 10129 Torino, Italy

<sup>c</sup> Department of Building and Real Estate, The Hong Kong Polytechnic University, Hung Hom, Kowloon, Hong Kong, China

## ARTICLE INFO

### Keywords:

Topology optimization  
Imperfection modeling  
Elasto-plastic analysis  
Reliability-based design

## ABSTRACT

In this paper, a novel optimization technique is implemented to explore the effects of considering uncertain load positions. Therefore, the integration of reliability-based design into structural topology optimization, while considering imperfect geometrically nonlinear analysis, is proposed. By comparing the results obtained from perfect and imperfect geometrically and materially nonlinear analyses, this study examines the impact of nonlinearity on probabilistic and deterministic analyses. Concerning probabilistic analysis, the originality of this research lies in its incorporation of the position of the applied load as a stochastic variable. This distinctive approach complements the consideration of other relevant parameters, including volume fraction, material properties, and geometrical imperfections, with the overarching goal of capturing the variability arising from real-world conditions. For the assessment of uncertainties, normal distribution is assumed for all these parameters. Normal distributions are chosen due to their advantages in terms of simplicity, ease of implementation, and computational efficiency. These characteristics are particularly beneficial when dealing with complex optimization algorithms and extensive analyses, as is the case in our research. The proposed algorithm is validated according to the results of benchmark problems. Structural examples like cantilever beam, pinned-shell, and L-shaped beam problems are further explored within the context of imperfect geometrically nonlinear reliability-based topology optimization, with specific regard to the probabilistic aspect of the location of the externally applied loads. Moreover, the results of the suggested approach suggest that the inclusion of a probabilistic design strategy has influenced topology optimization. The reliability index acts as a controlling constraint for the resulting optimized configurations, including the mean stress values associated with the resulting topologies.

## 1. Introduction

A mathematical technique known as topology optimization (TO) is utilized to optimize performance within predetermined constraints by distributing material in an efficient manner within a specified domain. This method has undergone considerable enhancements within the domain of structural engineering. Moreover, its effectiveness has been substantiated across an array of engineering disciplines, encompassing civil, mechanical, and other relevant applications, ultimately enhancing the innovative capabilities of designers [1–4].

TO has witnessed significant enhancements, leading to the emergence of various developmental techniques. One such method that has recently undergone substantial improvements is the bi-directional evolutionary structural optimization (BESO) method [5] known for its

unique ability to remove and add material based on sensitivity numbers. Several studies and works focused on the applications and developments of the BESO method, shedding light on its significance in the field of structural optimization [6–8]. For instance, Zhu et al. [9] presented an enhanced (BESO) approach for optimizing constrained layer damping, resulting in more rational and efficient layouts while maintaining damping effectiveness. Shobeiri [10] introduced an approach to enhance the effectiveness of numerical optimization techniques for nonlinear structures subjected to dynamic loads. The BESO approach was developed to improve contact stress uniformity by optimizing material stiffness, demonstrating its effectiveness in enhancing the contact stress distribution compared to interface shape optimization [11].

Regarding structural optimization, the consideration of structural stability has gained prominence alongside traditional factors such as

\* Corresponding author.

E-mail address: [majidmr@sze.hu](mailto:majidmr@sze.hu) (M. Movahedi Rad).

<https://doi.org/10.1016/j.istruc.2024.107533>

Received 19 July 2024; Received in revised form 1 October 2024; Accepted 9 October 2024

Available online 16 October 2024

2352-0124/© 2024 The Author(s). Published by Elsevier Ltd on behalf of Institution of Structural Engineers. This is an open access article under the CC BY license (<http://creativecommons.org/licenses/by/4.0/>).

strength and stiffness, with a growing emphasis on ensuring stability under varying conditions. This evolving perspective has garnered considerable interest in the examination and resolution of stability challenges, with a specific focus on intricate and complex structures, reflecting the extensive body of research that has already contributed to this vital area [12–15]. This leads to an examination of the interplay between topology optimization and structural stability, including methods, challenges, and advancements in this critical domain. Bian and Fang's [16] research concerned the optimization of three-dimensional structures involving buckling constraints. With the principal aim of optimizing the buckling load, Lindgaard et al. [17] presented an optimization technique for composite structures. Browne et al. [18] introduced a method for tackling large-scale binary programming problems in topology optimization with consideration of buckling constraints. Topology optimization approach of columns prone to stability loss by replacing conventional buckling load maximization with a locally formulated problem was proposed by Bochenek and Tajs-Zielińska [19]. Addressing the conflict between structural rigidity and stability requirements, Gao et al. [20] presented a continuation approach for optimizing the topology of structures.

In the field of structural engineering and design optimization, recent research efforts have delved into various methodologies to address uncertainties, ranging from reliability-based considerations and safety evaluations in straightforward engineering decisions to the optimization of complex components such as rotor blades and glulam beams. The work conducted by Papaioannou et al. [21], Drieschner et al. [22], Schmidt and Lahmer [23], and Schietzold et al. [24] has contributed significantly to the understanding of integrating polymorphic uncertainty frameworks, realistic uncertainty descriptions, and material-specific uncertainties into numerical structural designs. A topology optimization technique that takes hybrid uncertainties and manufacturing variables into account was proposed by Li et al. [25]. Additionally, Edler et al. [26] have explored optimization methodologies that incorporate uncertain structural parameters through the use of random variables and interval design parameters. By taking into account uncertainty in the location, direction, and amplitude of the applied load and properties of material, Li et al. [27] presented an effective reliability-based concurrent topology optimization.

Utilizing reliability-based topology optimization is an essential component in the ever-evolving domain of structural engineering. In order to ensure the resilience of structures in the face of the complex challenges presented by real-world dynamics, it is critical to thoroughly account for uncertainties, including variable load positions and other influential factors. As the pursuit of efficient structural designs through topology optimization continues to evolve, the consideration of reliability is emerging as an indispensable aspect of the optimization process. Reliability-based design seeks to enhance the robustness and safety of structures by incorporating probabilistic aspects, addressing uncertainties in materials [28], loads [29], and other parameters [30,31]. Habashneh and Movahedi [32] integrated reliability-based analysis into topology optimization, specifically focusing on geometrically nonlinear elasto-plastic models. Furthermore, Luo et al. [33] incorporated reliability-based design into stress-constrained topology optimization problems under numerous stress-related constraints. Jung and Cho [34] developed an optimization approach for probabilistic topology design problems with probabilistic displacement conditions. By considering three-dimensional structures, Eom et al. [35] proposed a reliability-based topology optimization (RBTO) approach with a focus on the stability of the structures.

As we navigate the intricate landscape of topology optimization (TO) and its integration with reliability-based design (RBD), we confront a pivotal factor that has the potential to influence structural performance – the inherent load uncertainties significantly. Acknowledging the probabilistic nature of applied loads, characterized by their stochastic variations and complex interactions with the structural response, becomes paramount to truly designing robust and reliable structures. This

focus area has garnered extensive research and investigation [36,37]. Bruggi et al. [38] introduced an optimization approach for composite structures incorporating homogenization-based topology optimization and addressing load uncertainty. Moreover, by considering random loads and a probabilistic compliance constraint, Lógó [39] presented a stochastic optimal topology design method. Gao et al. [40] introduced an effective approach for assessing load uncertainty in robust multi-material topology optimization problems.

Building on our prior research [41], the present work introduces an innovative refinement to the Bi-directional Evolutionary Structural Optimization (BESO) method. This work presents a novel computational algorithm that incorporates the probabilistic nature of load positions, leading to the formulation of a reliability-based topology optimization method tailored for geometrically nonlinear analyses of imperfect structures. The proposed methodology represents a significant advancement over existing techniques by not only addressing load position uncertainty but also extending the framework to include additional random variables, such as geometric imperfections, material properties, and volume fraction ( $V_f$ ). In practical engineering applications, exact load positions are often unknown, necessitating their treatment as uncertain variables. This inherent uncertainty induces variability in the structural response, potentially affecting the optimal designs derived through conventional topology optimization techniques. The numerical examples presented herein serve to illustrate the significant influence of load position uncertainty on the final optimized layouts of the structure, underscoring the importance of addressing this aspect in reliability-based design methodologies. The mentioned random variables are modeled with mean values and standard deviations, conforming to a normal distribution. The numerical examples explored serve to underscore the remarkable effectiveness and efficiency of the proposed methodology, highlighting its potential to make substantial contributions in the domain of topology optimization.

The subsequent sections of this manuscript are structured as follows: In Section 2, we present an overview of the theoretical foundation underpinning the proposed algorithm and the expanded BESO method. Section 3 provides a presentation of the numerical examples explored in this study. Lastly, Section 4 encompasses the conclusion, remarks, and future perspectives.

## 2. Theoretical framework: concepts and principles

In this section, a comprehensive overview of the problem background is presented laying the foundation for topology optimization. In order to account for material and geometric nonlinearity, this paper investigates both perfect and imperfect analyses utilizing shell bending theory. With a focus on stability-oriented design, the proposed work employs nonlinear finite element analysis to address imperfections in structures. The computational efficacy of the ABAQUS [42] software is utilized to address the sensitivity of imperfection. In the following subsections, methodologies for deterministic elasto-plastic topology optimization and probabilistic topology optimization are detailed. Following this, the algorithm that is suggested for implementation using the BESO method is presented, providing a succinct comprehensive manual for the development of designs that are both deterministic and probabilistic.

### 2.1. Overview of the finite element approach

This study explores the field of topology optimization by examining two distinct analyses. The first analysis, labeled perfect analysis that is materially and geometrically nonlinear (GMNA), hinges on the application of shell bending theory. Within this framework, a perfect structure is assumed, incorporating nonlinear large displacements and a law of completely nonlinear elasto-plastic hardening. In parallel, the secondary analysis, materially and geometrically nonlinear with imperfections (GMNIA) also draws from shell bending theory. GMNIA

accounts for elasto-plastic relationships and large displacements, introducing initial geometric imperfections in the proposed model as nodal displacements. It is important to note that geometric nonlinearity becomes significant in structures experiencing large deformations, especially in applications involving flexible or deformable materials, where the structural behavior deviates noticeably from linear models. Consequently, linear assumptions may lead to imprecise predictions. Similarly, the presence of material nonlinearity, resulting from the nonlinear relationship between stress and strain in materials, can have a substantial impact on the structural response, particularly beyond the point of yielding. This impact may lead to alterations in stiffness and deformation patterns. Understanding and accounting for these nonlinear effects is paramount for achieving a more reliable representation of the structural response under varying loading conditions.

In order to address the initial imperfections that emerge during the manufacturing process, stability-focused design necessitates the utilization of nonlinear finite element analysis. Predicted by Koiter's theory [43], experimental imperfection sensitivity patterns guide this consideration. Once the flawless structure has been scrutinized, the method of integrating imperfection during the post-analysis is demonstrated to be computationally efficient, thereby offering a cost-effective imperfection sensitivity analysis as well as low computational effort.

The utilization of ABAQUS [42] software enables this methodology, which assumes imperfections to be a linear eigenvectors combination derived from the linear buckling problem. The presented methodology does not purport to compute the minimum value of a collapsing load as resulting by an incremental analysis. Conversely, its emphasis is on investigating the response of an imperfect structure to topology optimization under probabilistic and deterministic conditions. Though the quest for evaluating the collapsing load value with imperfection remains an open topic in structural engineering as demonstrated by the numerous works presented in the literature [44,45], this work provides a unique perspective on topology optimization challenges.

The initiation of imperfect geometrically nonlinear and nonlinear material analysis in ABAQUS requires a structured approach. Begin by defining the geometric and material properties, incorporating parameters for nonlinear material behavior. Introduce initial geometric imperfections through nodal displacements, simulating real-world deviations. Crucially, precede the analysis with a linear buckling analysis to assess the structure's vulnerability to global buckling modes. This initial step establishes a foundation for subsequent nonlinear analyses, providing insights into potential modes of failure. Following the linear buckling analysis, leverage ABAQUS capabilities for geometrically nonlinear analysis, ensuring the model accurately represents large deformations. In nonlinear finite element analysis, the combined effects of material and geometric nonlinearities are accounted for. Rigorous validation against theoretical expectations and experimental data solidifies the comprehensive understanding of the structure's behavior under the influence of both geometric and material imperfections. It is imperative to emphasize that the detailed discussion regarding the model encompassing material nonlinearity will be expanded upon in Section 3.

## 2.2. Deterministic elasto-plastic topology optimization

In the context of plastic ultimate limit analysis, we address the evolution of elasto-plastic structure that is impacted by a steadily increasing force  $F_i$ . This one-parameter loading is expressed as:

$$F_i = m_i F_0 \tag{1}$$

Here,  $F_0$  denotes the initial applied force, and  $m_i$  is a scalar parameter known as the load multiplier. The gradual increase of  $m_i$  leads to the expansion of plastic zones within the body, eventually reaching a state of unrestricted plastic flow at extremely high intensities. The plastic limit state is achieved when the elastic limit load  $F_0$  is multiplied by the plastic ultimate load  $m_p$ , yielding  $F_p$ . The condition  $m_i - m_p \leq 0$  ensures

non-negativity of work done by external forces, aligning with the plastic limit state concept [46]. At the plastic limit state, the stresses and external forces are able to maintain the static equilibrium of the body. Therefore, the equilibrium equations will be used. In this analysis, we will examine the stress  $\sigma_{ij}$  in a body that is in quasi-static equilibrium with the plastic limit load.

$F_i = m_p F_0$ . Additionally, we will consider an arbitrary statically admissible stress and force  $\sigma_{ij}^s$  and  $F_{is} = m_i F_0$  that satisfy the yield condition [46]:

$$f(\sigma_{ij}^s, k) \leq 0. \tag{2}$$

In this case,  $k$  denotes the material's plastic properties. The principle of virtual velocities can be applied to the stress and force fields under consideration by utilizing the kinematically permissible strain rate  $\dot{\epsilon}_{ij}$  and velocities  $v_i$  and contemplating a deformable body with volume  $V$  and loading surface  $S_q$ :

$$\int_V \sigma_{ij} \dot{\epsilon}_{ij} dV = m_p \int_{S_q} F_0 v_i dS. \tag{3}$$

$$\int_V \sigma_{ij}^s \dot{\epsilon}_{ij} dV = m_i \int_{S_q} F_0 v_i dS. \tag{4}$$

Upon subtracting these two equations, the following expression is obtained:

$$\int_V (\sigma_{ij} - \sigma_{ij}^s) \dot{\epsilon}_{ij} dV = (m_p - m_i) \int_{S_q} F_0 v_i dS. \tag{5}$$

The normality rule and the convexity of the yield surface dictate that, at each location within the body:

$$(\sigma_{ij} - \sigma_{ij}^s) \dot{\epsilon}_{ij} \geq 0. \tag{6}$$

Eq. (5) therefore produces:

$$(m_p - m_i) \int_{S_q} F_0 v_i dS \geq 0. \tag{7}$$

Considering structural stability in optimization, the formulations of topology optimization for continuum structures based on elasto-plastic limit analysis is stated as follows:

$$\text{Minimize : } C = \frac{1}{2} \mathbf{f}^T \mathbf{u} = \mathbf{u}^T \mathbf{K} \mathbf{u}. \tag{8.a}$$

$$\text{Subject to : } V^* - \sum_{i=1}^N V_i x_i = 0. \tag{8.b}$$

$$x_i \in \{0, 1\}. \tag{8.c}$$

$$\lambda_j \geq \underline{\lambda} > 0. \tag{8.d}$$

$$m_i - m_p \leq 0. \tag{8.e}$$

Here, mean compliance, denoted as  $C$ , is quantified as the external work performed by applied loads or the total strain energy of the structure,  $\mathbf{u}$  signifies the displacement vector,  $\mathbf{K}$  denotes the global stiffness matrix, and  $\mathbf{f}$  represents the vector of force. Variables like  $V_i$ ,  $V^*$ , and  $x_i$  contribute to the constraints, reflecting element volume, total structure volume, and binary design considerations, respectively. The constraint  $(m_i - m_p \leq 0)$  emphasizes that the load multiplier  $m_i$  must be statically acceptable and equal to or less than the plastic ultimate load multiplier  $m_p$  corresponding to the entire domain. Moreover, Eq. (8.d) illustrates the constraint on buckling load factors, where  $\lambda_j$  represents the  $j$ -th buckling load factor associated with the provided load cases while  $\underline{\lambda}$  represents the minimum buckling load factor value.

For a comprehensive understanding of the BESO method, detailed descriptions and applied extensions are available in the existing literature [47–49]. This section also provides insights into path-dependent nonlinear problems and the incremental technique used for solving them. Sensitivity numbers, crucial for optimization, are modified iteratively. The procedure involves the extraction of a solid element, resulting in variations in overall strain energy or mean compliance, captured by the elemental sensitivity number ( $\alpha_i^e$ ) [50]:

$$\alpha_i^e = \Delta C_i = \frac{1}{2} \mathbf{u}_i^T \mathbf{K}_i \mathbf{u}_i. \tag{9}$$

Here,  $\mathbf{u}_i$  represents the nodal displacement, and  $\mathbf{K}_i$  stands for the stiffness matrix of the  $i$ -th element. Initial values of zero are assigned to the sensitivity of void elements.

The following terms characterize nodal sensitivity values ( $\alpha_j^n$ ) for nodes:

$$\alpha_j^n = \sum_{i=1}^M w_i \alpha_j^e, \tag{10}$$

where the number of elements coupled to the  $j$ -th node is denoted as  $M$ , and the weight factor  $w_i$  is expressed by:

$$w_i = \frac{1}{M-1} \left( 1 - \frac{r_{ij}}{\sum_{i=1}^M r_{ij}} \right), \tag{11}$$

where  $r_{ij}$  represents the distance between the  $j$ -th node and the center of the  $i$ -th element. Based on the aforementioned weight factor, the nodal sensitivity number is more significantly influenced by the elemental sensitivity number in proximity to the node. It will then be possible to convert the aforementioned nodal sensitivity values to averaged elemental sensitivity values. The process of conversion occurs via the projection of nodal sensitivity values onto the design domain.

To address issues related to checkerboard patterns in achieving optimal structures, a filter scheme is introduced [51]. The identification of nodes potentially affecting the sensitivity of the  $i$ -th element is facilitated by the utilization of  $r_{\min}$ . The enhanced elemental sensitivity number is determined as follows:

$$\alpha_i = \frac{\sum_{j=1}^B w(r_{ij}) \alpha_j^n}{\sum_{j=1}^K w(r_{ij})}. \tag{12}$$

where  $B$  represents the quantity of nodes contained in the sub-domain  $\Omega_i$ , while the linear weight  $w(r_{ij})$  factor is calculated as follows:

$$w(r_{ij}) = r_{\min} - r_{ij}. \tag{13}$$

To ensure stability in the evolutionary process, an averaging scheme is employed [52]:

$$\bar{\alpha}_i = \frac{\alpha_i^k + \alpha_i^{k-1}}{2}. \tag{14}$$

where  $k$  represents the current iteration number, and subsequently,  $\alpha_i^k = \bar{\alpha}_i$  for the succeeding iteration.

The equation utilized to calculate the target volume  $V_{k+1}$  for the subsequent iteration is:

$$V_{k+1} = V_k(1 \pm ER). \tag{15}$$

The value of  $ER$  denotes the evolutionary ratio, the selection of which is contingent upon the particular problem at hand and the intended degree of precision. This ratio regulates the rate of change between optimization process generations and can fluctuate depending on the nature of the problem and the optimization algorithm employed [50].

Following the fulfillment of the volume constraint, subsequent iterations do not affect the structural volume, as indicated by the expression:

$$V_{k+1} = V^*. \tag{16}$$

Then, the sorting of the elements is done based on their sensitivity numbers. Solid elements are deleted, while void elements are added according to the thresholds of their sensitivity values.

The convergence criteria that dictate the optimization procedure in BESO are defined in the subsequent manner:

$$error = \frac{|\sum_{i=1}^N (C_{k-i+1} - C_{k-N-i+1})|}{\sum_{i=1}^N C_{k-i+1}} \leq \tau. \tag{17}$$

In this context, the variable ( $k$ ) denotes the current iteration number, ( $C$ ) is the objective function,  $\tau$  represents the allowable convergence, which ensures that the optimization process halts when further iterations provide negligible improvements in the objective function, and ( $N$ ) is an integer value. Conventionally, the parameter  $N$  is set to 5, signifying that the observed change in mean compliance over the preceding 10 iterations is deemed acceptably small [50].

### 2.3. Probabilistic topology optimization

Considering uncertainties, especially in load positions, is critical for practical applications where structural responses must accommodate variations. This becomes particularly challenging when aiming for designs that can withstand these uncertainties. Several studies have delved into the challenging domain of topology optimization under uncertainties, addressing the complexities introduced by variations in load positions and environmental conditions [53,54]. Building upon the groundwork laid by previous studies in topology optimization under uncertainties, we delve into a specific scenario depicted in Fig. 1, where the applied load's position variability is a critical factor. As illustrated in the schematic diagram, the external load  $F$  is assigned to be applied in a manner where the position follows a random variable conforming to a Gaussian distribution characterized by a mean value  $\mu$  and standard deviation  $\sigma$ . Considering that  $\Gamma$  represents the boundary of structural domain  $\Omega$ . Thus, while the magnitude and direction of the external load  $F$  remain constant, it may adjust or move slightly within the boundary when applied precisely at a specific point.

The current technique of structural topology optimization should provide a layout design that is more reliable in order to eliminate or withstand variations in load positions. This will ensure that all applied forces are successfully transmitted to the restraint bounds. Evidently, this design optimization challenge is more challenging than the classic one with fixed load positions.

In reliability-based optimization, the probability of failure ( $P_f$ ) and the reliability index ( $\beta$ ) are critical indicators for assessing structural

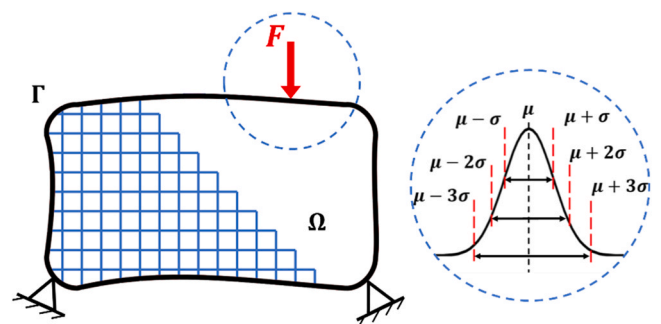


Fig. 1. Continuum structure under external force  $F$  applied at uncertain position within the boundary  $\Gamma$ .

performance under uncertainty. The reliability index,  $\beta$ , is a measure of the safety margin between the mean performance and the failure threshold, and it is inversely related to  $P_f$ , the probability that the structure will fail under specified conditions. The relationship between these two indicators is expressed as:

$$\beta = -\Phi^{-1}(P_f) \tag{18}$$

where  $\Phi^{-1}$  is the inverse of the cumulative distribution function (CDF) of the standard normal distribution. A higher  $\beta$  value corresponds to a lower  $P_f$ , indicating a more reliable structure. By estimating the probability of failure ( $P_f$ ), the reliability index ( $\beta$ ) is determined utilizing the Monte Carlo simulation procedure. The Monte Carlo simulation, as a general principle, solves problems by sampling realizations  $x$  from the probability function  $f_X(x)$  of the random vector  $X$ , relying on the concept of randomization. As a result, it is possible to estimate the  $P_f$  by estimation of the ratio of points inside the failure domain to the number of the total produced points [55]. An estimated value of the  $P_f$  ranging from  $10^{-7}$  to  $10^{-4}$  necessitates  $N = 10^6$  to  $10^9$  samples in order to ascertain the benefits (simplicity) of the Monte-Carlo simulation in order to derive the coefficient of variation  $\approx 0.1$ . Our method as a whole does not require a substantial amount of computation time, notwithstanding the time-consuming simulations involved. Therefore,  $N = 10^9$  samples have been chosen for our Monte Carlo simulation, we aimed to ensure a thorough exploration of the parameter space and achieve a reliable estimation of the coefficient of variation. This extensive sample size was chosen to maintain a robust representation of the underlying probability distribution [56].

Probabilistic approaches involve relevant parameters such as the position of the applied loads, material properties, imperfections, and  $V_f$ , in the form of random variables with mean and standard deviation. It is important to mention that this research adopts the Gaussian distribution model, also known as the normal distribution, which has been selected for its straightforwardness. It enables the calculation of the entire distribution using only two parameters: the mean and standard deviation. Furthermore, this distribution model is particularly well-suited for our study due to its widespread use in engineering and scientific contexts. Following this, by developing the  $\beta$ , it is possible to enforce the reliability constraint, which is related the  $V_f$  parameter as follows:

$$\beta_{\text{target}} - \beta_{\text{calc}} \leq 0. \tag{19}$$

To calculate  $\beta_{\text{target}}$  and  $\beta_{\text{calc}}$ :

$$\beta_{\text{target}} = -\Phi^{-1}(P_{f,\text{target}}). \tag{20}$$

$$\beta_{\text{calc}} = -\Phi^{-1}(P_{f,\text{calc}}). \tag{21}$$

By incorporating structural reliability indicators directly into the optimization formulation, uncertainties in the input variables are accounted for, resulting in designs that are reliable under probabilistic conditions. Therefore, the optimization problem is formulated as follows:

$$\text{Minimize : } C = \frac{1}{2} \mathbf{F}^T \mathbf{u} = \mathbf{u}^T \mathbf{K} \mathbf{u}. \tag{22.a}$$

$$\text{Subject to : } \mathbf{V}^n - \sum_{i=1}^N V_i x_i = 0 \tag{22.b}$$

$$x_i \in \{0, 1\} \tag{22.c}$$

$$\lambda_j \geq \underline{\lambda} > 0 \tag{22.d}$$

$$m_i - m_p \leq 0 \tag{22.e}$$

$$\beta_{\text{target}} - \beta_{\text{calc}} \leq 0 \tag{22.f}$$

Eqs. (22.a), (22.b), (22.c), (22.d), and (22.e) serve the same purpose

as Eqs. (8.a), (8.b), (8.c), (8.d), and (8.e) respectively. Additionally, Eq. (22.f) represents the reliability constraint related to  $V_f$ .

#### 2.4. The proposed algorithm utilizing BESO method

The BESO approach, renowned for its efficacy, shows itself to be a pragmatic option for topology optimization. The algorithm's overall performance is greatly enhanced by its distinctive capability to optimize according to sensitivity values. Subsequent to a succinct summary of the mathematical attributes of the novel problem, the algorithmic procedure illustrated in Fig. 2 can be utilized to formulate designs that are both deterministic and probabilistic.

The finite element simulations were conducted using ABAQUS, with MATLAB employed to handle the optimization process and data interaction. MATLAB calls the ABAQUS solver through system commands, utilizing an input file that contains the FE model's geometry, boundary conditions, and load cases. After running the simulation in ABAQUS, the output data, stored in an output database file, is processed by MATLAB. Custom MATLAB scripts were developed to extract relevant response variables such as stresses, displacements, and reaction forces from the ABAQUS output database. These values are then fed back into the optimization loop to adjust the parameters for subsequent simulations.

The flow chart can be concluded by the following steps:

1. Establishing BESO parameters.
2. Specifying probabilistic parameters for relevant random variables.
3. Model specification, encompassing load conditions and boundary parameters.
4. Implementing finite element simulation: performing linear buckling analysis, followed by incorporating model imperfections.
5. Calculating nodal and elemental sensitivities, followed by the application of enhancement schemes.
6. Specifying the  $\beta_{\text{target}}$  for probabilistic designs or the volume required for subsequent iterations, respectively, in the case of deterministic designs.
7. Estimating  $P_f$  and  $\beta_{\text{target}}$  values, by choosing  $N = 10^9$  samples for our Monte Carlo simulation to ensure a comprehensive exploration of the parameter space and to achieve a reliable estimation of the coefficient of variation.
8. Iterate through steps 3–7 until the defined constraints are met and convergence criteria, as specified in Eq. (17), are satisfied.

#### 3. Numerical examples

This section provides an analysis of three numerical examples to demonstrate the effectiveness of the proposed reliability-based GMNA and GMNIA optimization algorithm which considers the position of the applied load, material properties,  $V_f$ , and geometrical imperfections as random variables following normal distribution. The first two examples are slender cantilever and slender shell problems which are considered as benchmark problems that have been done by Movahedi et al. [41], while the third example is an L-shape beam problem.

The Monte Carlo simulation is employed to model the probabilistic nature of the problem. The presented method illustrates the suitability of the provided algorithm in obtaining reliable results with relative ease.

Stimulating imperfections with linear buckling modes allows for the consideration of both local and global buckling effects. The choice of buckling modes during the optimization procedure can have a substantial impact. When a structure reaches its critical load, it exhibits distinct deformation patterns known as buckling modes. The optimization procedure may struggle to converge towards an optimal solution if the selected buckling modes do not accurately represent the structural behavior.

In this study, the finite element analysis was conducted using ABAQUS software, employing the (S4) elements for mesh discretization. The (S4) elements are a type of quadrilateral plane stress element, commonly

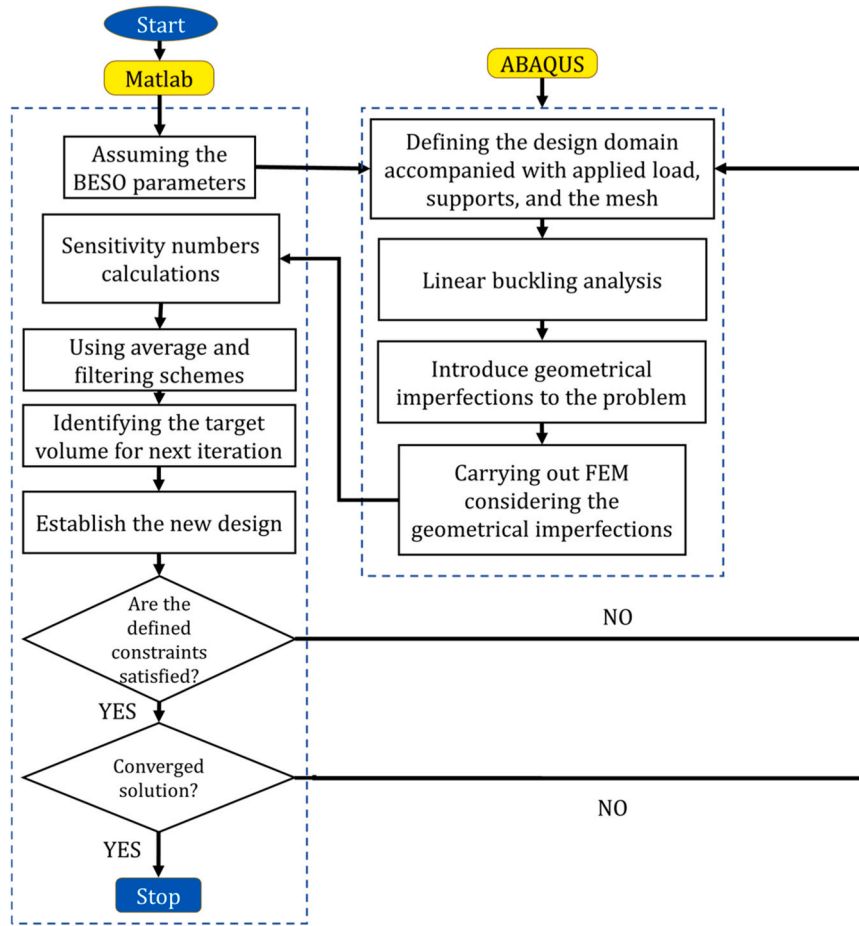


Fig. 2. The process of the proposed algorithm.

used for modeling thin structures subjected to in-plane loading. These elements are characterized by their capability to accurately capture bending and membrane effects, making them well-suited for applications in structural and mechanical engineering. The (S4) elements offer a balance between computational efficiency and accuracy, making them a suitable choice for the numerical simulations for the purpose of the current research. Additionally, we examine the impact of mesh size variations on the sensitivity of our optimization outcomes, given the pivotal significance of this parameter in determining the precision, convergence, and reliability of our simulations. Therefore, each instance examined in our research includes justifications for the selected element mesh size.

In the context of the GMNA and GMNIA models, to analyze the nonlinear stress-strain characteristics of aluminum alloy, the Ramberg-Osgood formulation is utilized, as suggested by Yun et al. [57]. This formulation is encapsulated in Eqs. (23–24):

$$\varepsilon = \frac{\sigma}{E} + 0.002 \left( \frac{\sigma}{f_y} \right)^n \text{ for } \sigma \leq f_y \quad (23)$$

$$\varepsilon = 0.002 + \frac{f_y}{E} + \frac{\sigma - f_y}{E_y} + \varepsilon_u \left( \frac{\sigma - f_y}{f_u - f_y} \right)^m \text{ for } f_y < \sigma \leq f_u \quad (24)$$

Here,  $\sigma$  denotes stress, and  $\varepsilon$  signifies strain. The parameters include yield (0.2 % proof) stress ( $f_y$ ), ultimate stress ( $f_u$ ), Young’s modulus ( $E$ ), strain hardening exponents ( $n$  and  $m$ , representing the first and second values, respectively), and ultimate strain ( $\varepsilon_u$ ). The tangent modulus ( $E_y$ ) at the yield stress is defined by:

$$E_y = \frac{E}{1 + 0.002n \frac{E}{f_y}} \quad (25)$$

Within the scope of this paper, we focus on a specific curve of stress and strain for a grade of aluminum alloy (6061–T6) in the context of numerical examples. The material properties are set as follows [58]:

$E = 70,200\text{N/mm}^2$ ,  $f_u = 222\text{N/mm}^2$ ,  $n = 15$ , and  $f_y = 192\text{N/mm}^2$ . The values for  $\varepsilon_u$  and  $m$  are determined using Eqs. (26) and (27), respectively. Furthermore, to introduce an element of reliability, we depart from deterministic and treat material property parameters as random variables, incorporating them as mean values with standard deviation value of 5% into the analysis.

$$\varepsilon_u = 1 - \frac{f_y}{f_u} \quad (26)$$

$$m = 1 + 3.5 \frac{f_y}{f_u} \quad (27)$$

### 3.1. Example #1: slender cantilever

The study commences by illustrating a numerical example of topology optimization. In this example, a shell cantilever is considered with fixed boundary conditions at the left end, ensuring that no displacement or rotation is allowed at that point. The optimization employs the GMNIA approach, incorporating the BESO technique for both deterministic and probabilistic designs.

The results of this example are validated according to Movahedi et al. [41], then evaluating the outcomes of the suggested algorithm by taken

into account the additional random variable which is related to the uncertainty of the position of the applied load. The thickness of the considered slender cantilever is 25 mm. Fig. 3 illustrates the design domain of the considered problem. Furthermore, for the finite element analysis, a detailed mesh division is applied to the design domain. The thickness of the slender cantilever is 25 mm, and the dimensions of the cantilever are 1000 mm in length and 250 mm in width. The design domain is discretized into 10,000 elements of S4 shell elements, which are chosen for their ability to accurately model the bending and twisting behaviors of shell structures. A mesh element size of 5 mm is utilized, ensuring a refined representation of the geometry and accurate results in the optimization process.

The beam's initial specified load is equal to  $F_0 = 20\text{kN}$ . The load multiplier under consideration is  $m_i = 2$ , whereas the load multiplier for the plastic limit is  $m_p = 4.05$ . As shown in Fig. 3, the acting force  $F = m_i F_0 = 40\text{kN}$  is therefore deemed to be responsible for the plastic stress. This force is spread within the elements by means of plastic analysis. Taking into account that the ultimate load is  $F_{ult} = m_p F_0 = 81\text{ kN}$ . Furthermore, loads are distributed across multiple elements or nodes in order to prevent local yielding.

The following BESO parameters are taken into account for this problem:  $ER = 1\%$ , a prescribed maximum volume addition ratio ( $AR_{max} = 1\%$ ),  $r_{min} = 20\text{ mm}$  and  $\tau = 0.5\%$ . The  $V_f$  is 62%. Furthermore, the GMNIA algorithm takes into account the imperfection value as  $L/1000$  for the initial linear buckling mode and  $b/250$  for the second mode. The eigenmodes themselves are normalized such that the maximum absolute value of the mode shape is set to unity. The Monte-Carlo technique is employed here. For the purpose of reliability assessment, the position of the applied load, geometric imperfection, material properties, and  $V_f$  are considered stochastic variables to capture the probabilistic nature of the analysis. Furthermore, Fig. 4 shows the considered normal distribution of the uncertain load position. Also,  $N = 10^9$ . The initial two eigenmodes depicted in the benchmark problem are shown in Fig. 5. Table 1 shows the additional considered random variables.

Table 2 displays a comparison of the deterministic design findings for optimized layouts and mean stresses of the model between GMNA and GMNIA. The insights derived from the data presented in Table 2 demonstrate that when considering deterministic designs, the mean stress values for GMNIA are greater than those for GMNA. Specifically, the mean stress is elevated by 2.52% from 67.70 MPa in the case of GMNA to 69.45 MPa in the case of GMNIA.

Based on the final optimized forms of the two scenarios (GMNA and GMNIA), it can be concluded that there is little change in the optimum topological shapes when considering  $V_f = 0.62$ .

The results of incorporating reliability-based topology optimization are presented in Fig. 6 by considering  $\beta_{target} = 3.14$ ,  $P_{f,target} = 8 \cdot 10^{-4}$ . Additionally, it is important to highlight that this comparison incorporates the consideration of uncertain load positions, building upon the work conducted by Movahedi et al. [41]. In the deterministic framework, the design process relies on the assumption of a fixed, precisely known load application point. This simplification, while convenient, introduces a trade-off in the design. On one hand, it tends to lead to conservative designs as it does not explicitly account for potential

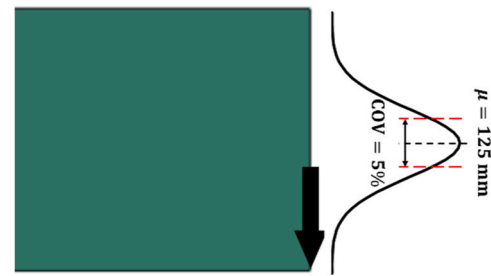


Fig. 4. Normal distribution of the loading position.

variations in load position due to uncertainties, inaccuracies, or real-world conditions. On the other hand, the designs may also be more sensitive to variations that are not taken into account. This dual nature of the simplification highlights the complexity in balancing conservatism and sensitivity in the design process. Conversely, the reliability-based approach, as employed in our study, adopts a more realistic viewpoint by acknowledging that the load position is subject to variability and uncertainty, allowing for a more comprehensive assessment of structural performance. As it can be seen from the results from Fig. 6, The resulting optimized layouts under the reliability-based framework exhibit variations that are a direct consequence of this broader perspective.

The results in Table 3 indicates another comparison that is made based on the values of the mean stress of the optimum layout resulting from the proposed algorithm in addition to the resulted topologies which were done according to Movahedi et al. [41]. The results of the proposed algorithm reveal a 3.79% increase in mean stress, rising from 65.90MPa in the case of GMNA to 68.40MPa in the case of GMNIA. In essence, when accounting for stochastic variables such as material properties, applied load position, geometric imperfections, and  $V_f$ , the disparities between the outcomes of GMNA and GMNIA scenarios become more pronounced, surpassing the differences observed in deterministic design results. This increment in mean stress signifies the substantial influence of incorporation of the previously mentioned random variables into the optimization problem. The higher mean stress observed with the proposed GMNIA method (68.40 MPa) compared to the results of Movahedi et al. [41] for GMNIA (67.88 MPa), it is essential to emphasize the advantages of the GMNIA approach within a probabilistic framework. While both methods account for uncertainties, the increase in mean stress signifies a more effectively optimized design that strategically allocates material to withstand variations in load positions and material properties. This optimization leads to layouts that exhibit enhanced structural resilience and material efficiency, allowing the design to better accommodate real-world operational conditions. Furthermore, as illustrated in Fig. 6, the higher stress values can be interpreted as a result of strategically placing material in regions where it can best resist applied forces, optimizing material usage while ensuring the structure's integrity under operational conditions.

### 3.2. Example #2: thin shell problem

The second numerical example focuses on the optimization of a thin shell. The shell is anchored at both extremities' centers, and the boundary conditions are set to prevent any movement or rotation at these anchor points. Also, as mentioned earlier in previous examples, Monte-Carlo simulation is used. For the purpose of reliability assessment, material properties, the position of the applied load, geometric imperfection, and  $V_f$  are considered stochastic variables to capture the probabilistic nature of the analysis.

For the finite element analysis, the design domain is discretized into 6400 S4 shell elements. These elements are selected due to their ability to accurately capture the bending, shear, and membrane behavior inherent in thin shell structures. The S4 element is a four-node, shell

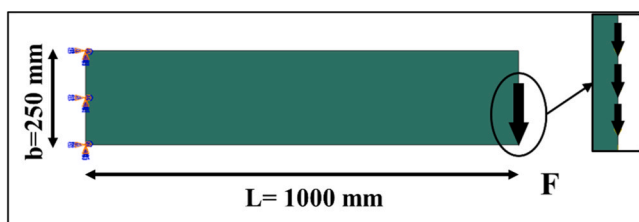


Fig. 3. Slender cantilever problem.

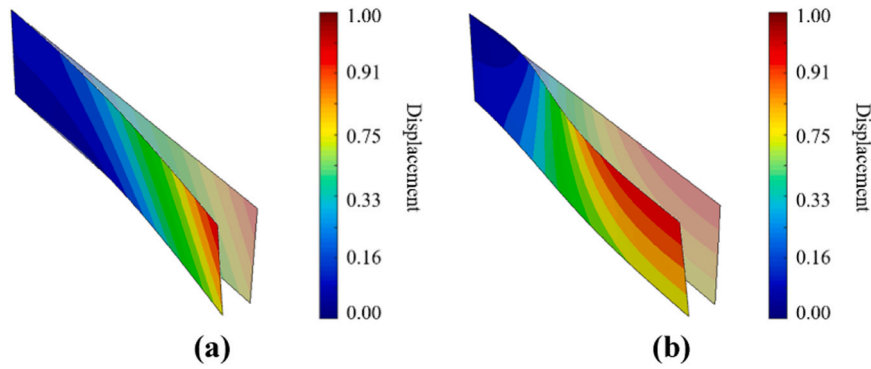


Fig. 5. Slender cantilever’s linear buckling modes: (a) first mode (b) second mode.

**Table 1**  
Considered random variables.

Parameter	Mean value	COV
$V_f$	0.62	5.00%
$L/1000$ (mm)	1.00	
$E$ (MPa)	70,200	

finite element that allows for the representation of complex geometries while maintaining computational efficiency. The mesh is generated with a size of 5 mm, which is a critical parameter for ensuring sufficient detail in the numerical analysis. This element size balances computational cost and solution accuracy, allowing for precise modeling of stress distribution and deformation patterns under applied loads.

Fig. 7 illustrates the design domain of the considered shell. Furthermore, the length of the considered example is 800 mm and the width is 200 mm. The shell’s initial specified load is equal to  $F_0 = 15\text{kN}$ .

**Table 2**  
Optimization results under deterministic conditions for the slender cantilever.

$V_f = 0.62$	GMNA	GMNIA
Optimized layout		
Mean stress (MPa)	67.70	69.45

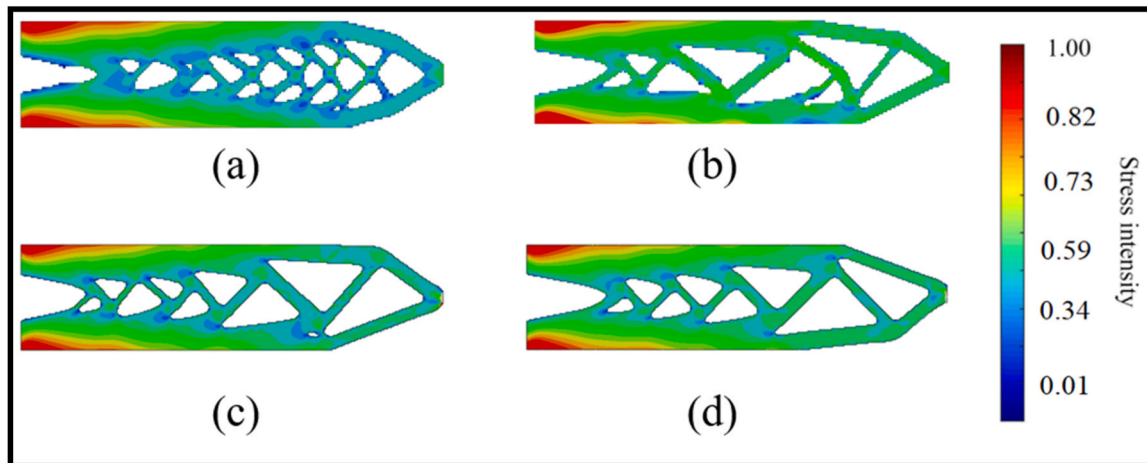


Fig. 6. The resulted optimal topologies in the case of  $\beta_{target} = 3.14$ : (a) GMNA [41] (b) GMNIA [41] (c) GMNA – proposed algorithm (d) GMNIA – Proposed algorithm.

**Table 3**  
The obtained values of mean stress of the slender cantilever model.

Algorithm	Model	Mean stress (MPa)
Movahedi et al. [41]	GMNA	58.50
	GMNIA	67.88
The proposed work	GMNA	65.90
	GMNIA	68.40

**Table 4**  
Considered random variables.

Parameter	Mean value	COV
$V_f$	0.62	5.00%
$L/1000$ (mm)	0.80	
$E$ (MPa)	70,200	

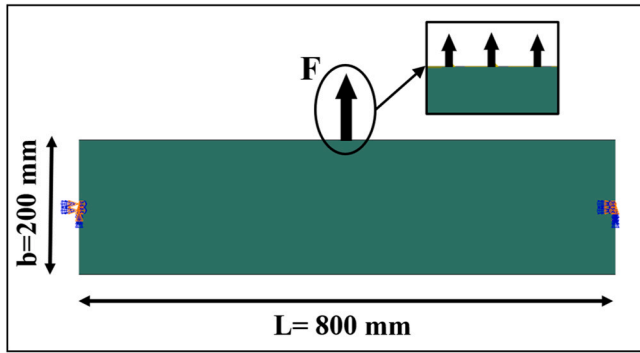


Fig. 7. Thin shell problem.

The load multiplier under consideration is  $m_i = 4$ , whereas the load multiplier for the plastic limit is  $m_p = 4.05$ . As shown in Fig. 3, the acting force  $F = m_i F_0 = 60\text{kN}$  is therefore deemed to be responsible for the plastic stress. This force is spread within the elements by means of plastic analysis. Taking into account that the ultimate load is  $F_{ult} = m_p F_0 = 60.75\text{ kN}$ . The following BESO parameters are taken into account for this problem:  $ER = 1\%$ ,  $AR_{max} = 1\%$ ,  $r_{min} = 20\text{mm}$  and  $\tau = 0.5\%$ . The considered value of  $V_f$  is 62%. Furthermore, the GMNIA algorithm takes into account the imperfection value as  $\frac{L}{1000}$  for the initial linear buckling mode and  $\frac{b}{300}$  for the second mode. The Monte-Carlo technique is employed here. For the purpose of reliability assessment, material properties, the position of the applied load, geometric imperfection, and  $V_f$  are considered stochastic variables to capture the probabilistic nature of the analysis. Furthermore, Fig. 4 shows the considered normal distribution of the uncertain load position.  $N$  is considered  $10^9$ . The initial two eigenmodes depicted in the benchmark problem are shown in Fig. 8. In Table 4, the additional random variables under consideration can be found.

As described in Section (3.1), the first two eigenmodes are considered for both global and local buckling in the linear buckling analysis.

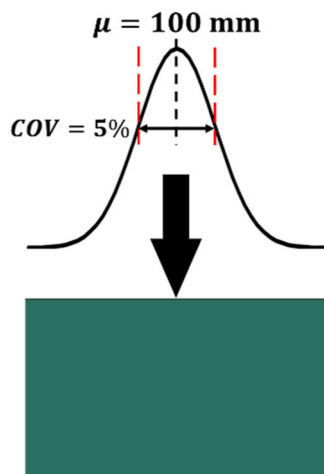


Fig. 8. The considered normal distribution of the loading position.

These two modes of the illustrated example are depicted in Fig. 9.

Table 5 displays a comparison of the deterministic design findings for optimized layouts and mean stresses of the model between GMNA and GMNIA. The findings from Table 3 demonstrate that when considering deterministic designs, the mean stress values for GMNIA are greater than those for GMNA. Specifically, the mean stress is elevated by 1.94% from 77.63 MPa in the case of GMNA to 79.14 MPa in the case of GMNIA. Based on the final optimized forms of the two instances (GMNA and GMNIA), it can be concluded that there are observable changes in the optimum topological shapes when considering  $V_f = 0.60$ .

The results of incorporating reliability-based topology optimization are presented in Fig. 10 by considering  $\beta_{target} = 3.18$ ,  $P_{f,target} = 9 \cdot 10^{-4}$ . It should be noted that in addition to what was previously done by Movahedi et al. [41], the results of considering uncertain load position is considered in this comparison also. In the deterministic framework, the design process hinges on the assumption of a fixed, precisely known load application point. This simplification, while convenient, tends to lead to conservative designs, as it does not account for potential variations in load position due to uncertainties, inaccuracies, or real-world conditions. Conversely, the reliability-based approach, which has employed, adopts a more realistic viewpoint by acknowledging that the load position is subject to variability and uncertainty. As it can be seen from the results from Fig. 10, The resulting optimized layouts under the reliability-based framework exhibit variations that are a direct consequence of this broader perspective.

The results in Table 6 indicates another comparison that is made based on the values of the mean stress of the optimum layout resulting from the proposed algorithm in addition to the resulted topologies which were done according to Movahedi et al. [41]. It can be noticed that the results of the proposed algorithm indicate that the mean stress is increased by 8.68% from 72.40 MPa in case of GMNA to 78.69 MPa in case of GMNIA. In other words when material properties, the position of the applied load, geometric imperfection, and  $V_f$  are considered stochastic variables, The differences in the outcomes of both GMNA and GMNIA scenarios are more substantial when compared to the deterministic design results. This increment in mean stress signifies the substantial influence of incorporation of the previously mentioned random variables into the optimization problem.

### 3.3. Example #3: L-shaped beam

The third numerical example addresses a topology optimization problem for an L-shaped beam. The beam is fixed at the top end, imposing constraints to restrict any displacement or rotation at that specific location. The results of this example in the case of deterministic and probabilistic GMNA are validated according to Movahedi et al. [59], then the results of the proposed algorithm of GMNA and GMNIA by considering additional random variable which is related to the uncertainty of the position of the applied load is discussed.

Fig. 11 depicts the design domain of the considered problem, which is discretized into 3900 S4 shell elements, that are particularly well-suited for modeling the L-shaped beam due to their capacity to accurately represent complex geometries and capture bending and shear effects. The S4 elements are four-node shell elements that facilitate efficient computations while ensuring high fidelity in the analysis. A 5 mm mesh size is selected to strike a balance between computational efficiency and solution accuracy. This size allows for a detailed representation of the stress distribution and deformation patterns, critical for

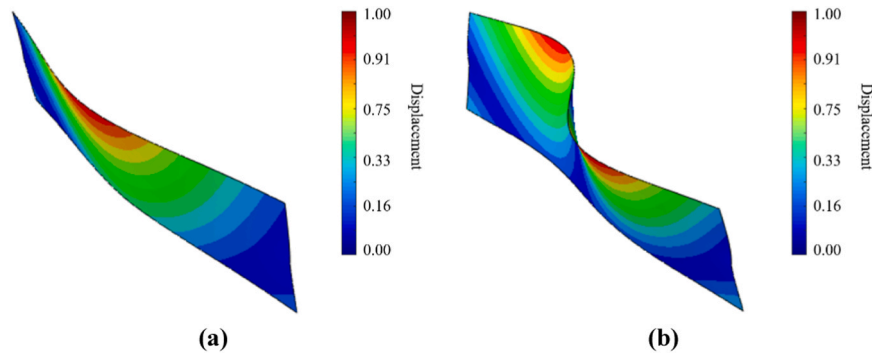


Fig. 9. Thin shell's linear buckling modes: (a) first mode (b) second mode.

Table 5  
Optimization results under deterministic conditions for the thin shell.

$V_f = 0.60$	GMNA	GMNIA
Optimized layout		
Mean stress (MPa)	77.63	79.14

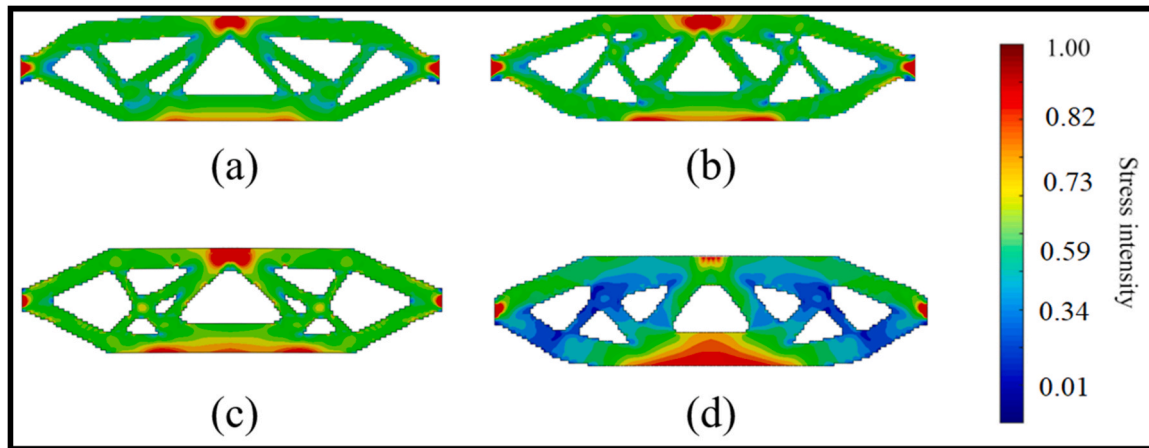


Fig. 10. The resulted optimal topologies in the case of  $\beta_{target} = 3.18$ : (a) GMNA – without considering uncertain load position [41] (b) GMNIA – without considering uncertain load position [41] (c) GMNA – proposed algorithm (d) GMNIA – Proposed algorithm.

Table 6  
The obtained values of mean stress of the slender cantilever model.

Algorithm	Model	Mean stress (MPa)
Movahedi et al. [41]	GMNA	73.92
	GMNIA	78.54
The proposed work	GMNA	72.40
	GMNIA	78.69

an accurate optimization process. The uniformity and quality of the mesh are essential, particularly in regions where stress concentrations are expected, such as at the constraints and load application points. Furthermore, the length of the considered example is 1000 mm and the width is 250 mm. The initial magnitude of the applied load on the beam is equal to  $F_0 = 4\text{kN}$  while yield stress equals  $\sigma_y = 110\text{MPa}$  and the Poisson's ratio was considered to be 0.3 for the elasto-plastic analysis. The plastic limit load multiplier  $m_p = 4.25$ , for the whole design domain. For the whole design domain, the plastic ultimate load

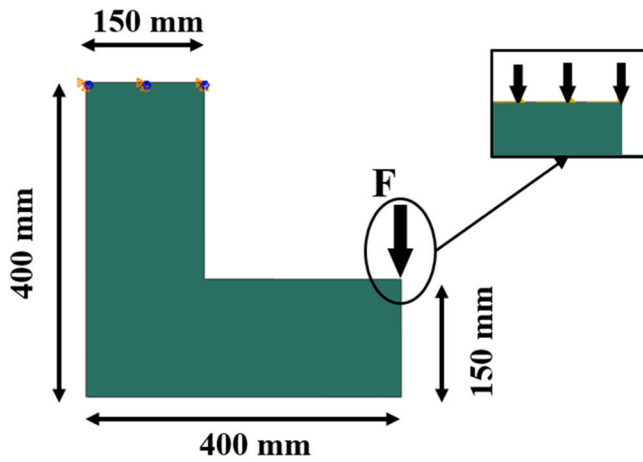


Fig. 11. L-shaped problem.

multiplier  $m_p = 4.25$ . Hence, the operating force under consideration that is accountable for the plastic stresses is  $F = m_i F_0 = 12\text{kN}$ , as demonstrated by the application of plastic analysis, which distributes it among the elements as it is shown in Fig. 11. The ultimate force is  $F_{ult} = m_p F_0 = 17\text{ kN}$ . Thickness of 10 mm are assumed. The BESO parameters taken into consideration for this problem are as following:  $AR_{max} = 1\%$ ,  $\tau = 0.1\%$ ,  $r_{min} = 18\text{ mm}$ , and  $ER = 1\%$ . Also, the value that is being considered for  $V_f$  is 40%.

Moreover, the GMNIA algorithm takes into account the imperfection value as  $L/1000$  for the initial linear buckling mode. The Monte-Carlo technique is employed here. For the purpose of reliability assessment, material properties, the position of the applied load, geometric imperfection, and  $V_f$  are considered stochastic variables to capture the probabilistic nature of the analysis. Furthermore, Fig. 12 illustrates the chosen distribution for the uncertain load position, modeled as a truncated normal distribution with constraints on the left side, taking into consideration that  $N = 10^9$ . The initial eigenmode depicted in the problem is shown in Fig. 13. The random variables considered additionally are presented in Table 7.

The considered eigenmode in the linear buckling step of the L-shaped problem is illustrated in Fig. 13. Table 5 presents a comparison between deterministic and probabilistic design results for the GMNA of the optimized shapes. The findings in Table 8 indicate significant differences in the resulting optimized shapes between deterministic and probabilistic designs. Additionally, the region containing the yielded elements in the optimal shape has been significantly reduced in the case of

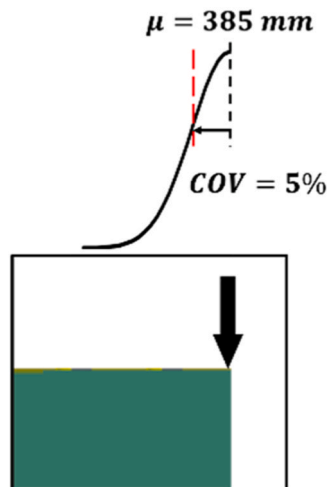


Fig. 12. The considered truncated normal distribution of the loading position.

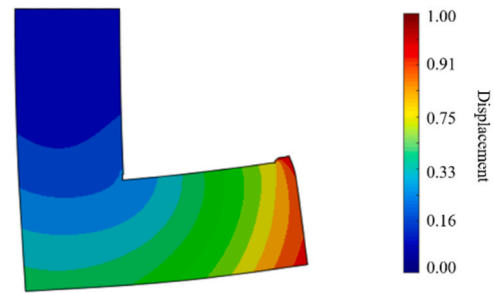


Fig. 13. Linear buckling mode for the L-shaped beam.

Table 7  
Considered random variables.

Parameter	Mean value	COV
$V_f$	0.40	5.00%
$L/1000$ (mm)	0.40	
$E(\text{MPa})$	70,200	

probabilistic designs compared to that in deterministic designs.

The results of incorporating reliability-based topology optimization by considering GMNA and GMNIA are presented in Fig. 14 by considering  $\beta_{target} = 3.79$ . Taking into consideration that the load position,  $V_f$ , geometrical imperfections and material properties are assumed to be random variables following normal distribution.

In the deterministic framework, the design process hinges on the assumption of a fixed, precisely known load application point. This simplification, while convenient, tends to lead to conservative designs, as it does not account for potential variations in load position due to uncertainties, inaccuracies, or real-world conditions. Conversely, the reliability-based approach, which has employed, adopts a more realistic viewpoint by acknowledging that the load position is subject to variability and uncertainty. As it can be seen from the results from Fig. 14, The resulting optimized layouts under the reliability-based framework exhibit variations that are a direct consequence of this broader perspective.

The results in Table 9 indicates another comparison that is made based on the values of the mean stress of the optimum layout resulting from the proposed algorithm. It can be noticed that the results of the proposed algorithm indicate that the mean stress is increased by 8.27% from 47.40 MPa in case of GMNA to 51.32 MPa in case of GMNIA. Put simply, the disparities between the outcomes of the two scenarios (GMNA and GMNIA) become more pronounced when you take into account material properties, uncertain load position,  $V_f$ , and initial geometric imperfection random variables. The observed increase in average stress indicates that the inclusion of the aforementioned stochastic variables in the optimization problem had a significant impact.

3.4. Results overview and computational efficiency

The results uncovered in this research, which clarify the discrepancies between probabilistic and deterministic structural designs, have significant implications for the discipline of structural engineering. By analyzing the distinctions between probabilistic and deterministic designs in the contexts of a thin shell, slender cantilever, and L-shaped beam, the research highlights the profound effect that implementing a reliability-based methodology can have. Adapted to load position uncertainties, material property uncertainties, and geometric imperfections, the algorithm represents a paradigm shift in topology optimization.

Engineers and designers in pursuit of reliable and practical optimized structures will find the presented algorithm to be a potent instrument due to its adaptability to a wide variety of structural configurations.

**Table 8**  
Optimized results of L-shaped beam.

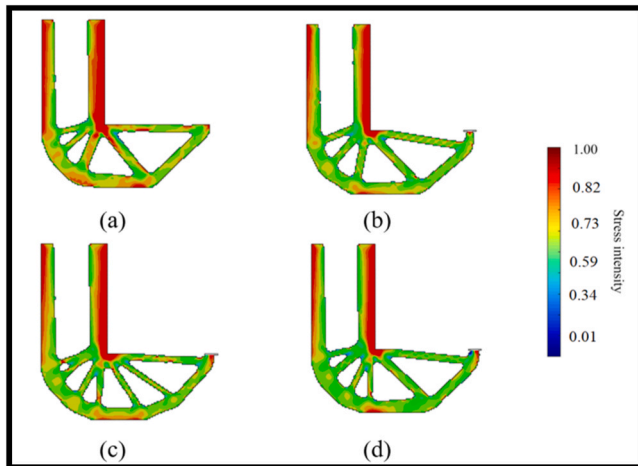
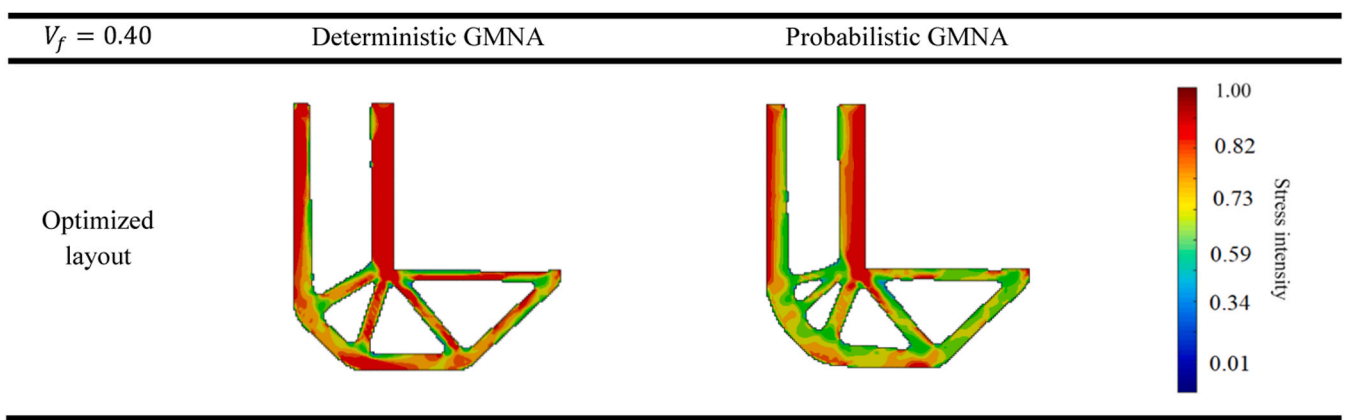


**Fig. 14.** The resulted optimal topologies in the case of  $\beta_{target} = 3.79$ ,  $P_{f,target} = 7 \cdot 10^{-5}$ . : (a) GMNA – without considering uncertain load position (b) GMNIA - without considering uncertain load position (c) GMNA – proposed algorithm (d) GMNIA – Proposed algorithm.

**Table 9**  
The obtained values of mean stress of the L-shaped problem.

Algorithm	Model	Mean stress (MPa)
Without considering uncertain load position	GMNA	48.20
	GMNIA	50.47
The proposed work	GMNA	47.40
	GMNIA	51.32

Although the algorithm demonstrates remarkable effectiveness in various structural configurations, it is crucial to moderately recognize its limitations. Future research efforts should prioritize the refinement of the algorithm’s complexities, which acknowledges the necessity for a more thorough discourse on its limitations.

Since computational efficiency criteria play a significant role in the optimization process, it is noteworthy to mention that the topology optimization was executed on a personal computer equipped with an Intel® Core™ i7–7700HQ @2.80 GHz processor and 16.0 GB RAM. The CPU time required for each model in the proposed reliability-based topology optimization method is detailed in [Table 10](#).

**Table 10**  
Computation time required.

TO problem	CPU time for the whole optimization process (second)	
	GMNA	GMNIA
Slender cantilever problem	7560	7740
Thin shell problem	3840	4020
L-shaped beam problem	5400	5700

#### 4. Conclusions

In this paper, a novel reliability-based structural topology optimization algorithm was developed, integrating the concepts of perfectly structures considering geometrically and materially nonlinear analysis (GMNA) and imperfectly structures considering geometrically and materially nonlinear analysis (GMNIA). The algorithm extends its capabilities by considering the position of the applied load, treating it as a stochastic variable within the framework of probabilistic analysis. Our algorithm’s effectiveness is showcased across a diverse range of structural configurations, including slender cantilevers, shells, and L-shaped beams. This versatility underscores its potential applicability to a broad spectrum of engineering designs. Furthermore, the consideration of  $V_f$  in our algorithm not only impacts structural efficiency but also holds eco-friendly implications. The optimization process inherently promotes resource conservation by minimizing material usage while maintaining structural integrity.

The essential findings constituting the conclusion of this study include:

- The incorporation of uncertain load positions and other random variables reveals substantial changes in optimized shapes and mean stresses. Therefore, it can be said that sensitivity to uncertainties is notably highlighted in the probabilistic design, with variations becoming more pronounced compared to deterministic design.
- The introduction of reliability-based design, considering random variables such as position of the applied load,  $V_f$ , geometric imperfections, and material properties, results in remarkable differences between GMNA and GMNIA outcomes.
- This approach offers practical and robust solutions for structural topology optimization, surpassing the conservatism observed in deterministic designs.

The outcomes of the proposed algorithm highlight the significance of considering uncertainties in topology optimization. The deterministic designs, while useful, tend to be conservative. In contrast, the reliability-

based approach, with its consideration of uncertain load positions and other variables, offers practical and robust solutions for structural topology optimization. The presented algorithm demonstrates its versatility across different structural configurations, making it a valuable tool for engineers and designers seeking efficient and reliable optimized structures. Furthermore, the interdisciplinary nature of our research positions the reliability-based algorithm as a valuable asset not only in structural engineering but also in related fields. Its adaptability could extend to disciplines like aerospace, automotive, and beyond. While this study successfully introduced a reliability-based algorithm for structural topology optimization, future research could delve into refining and expanding the algorithm's capabilities. Further investigations may include the consideration of additional uncertainties, optimization under dynamic loads, and the application of the algorithm to more complex structures. Future research could include cross-validation through industry case studies, allowing the algorithm's real-world performance to be tested in diverse engineering applications. This step would further validate its reliability and effectiveness in practical settings. Furthermore, future research could focus on extending our methodology to accommodate uncertainties in Dirichlet boundary conditions, such as uncertain displacement values or fixation positions.

### CRedit authorship contribution statement

**Raffaele Cucuzza:** Writing – review & editing, Validation, Methodology, Formal analysis, Conceptualization. **Muayad Habashneh:** Writing – original draft, Methodology, Conceptualization. **Majid Movahedi Rad:** Writing – review & editing, Validation, Supervision, Software, Conceptualization. **Peyman Aela:** Writing – review & editing, Visualization, Investigation.

### Declaration of Competing Interest

The authors declare that they have no known competing financial interests or personal relationships that could have appeared to influence the work reported in this paper.

### Data availability

The datasets utilized and/or generated throughout this work are included in the main manuscript.

### References

- Lim J, You C, Dayyani I. Multi-objective topology optimization and structural analysis of periodic spaceframe structures. *Mater Des* 2020;190:108552. <https://doi.org/10.1016/j.matdes.2020.108552>.
- Deng X, Chen H, Xu Q, Feng F, Chen X, Lv X, et al. Topology optimization design of three-dimensional multi-material and multi-body structure based on irregular cellular hybrid cellular automata method. *Sci Rep* 2022;12:1–20. <https://doi.org/10.1038/s41598-022-09249-y>.
- Niu B, Liu X, Wallin M, Wadbro E. Topology optimization of compliant mechanisms considering strain variance. *Struct Multidiscip Optim* 2020;62:1457–71. <https://doi.org/10.1007/S00158-020-02632-1/FIGURES/15>.
- Liang QQ, Xie YM, Prentice Steven G. Topology optimization of strut-and-tie models in reinforced concrete structures using an evolutionary procedure. *Struct J* 2000;97:322–30. <https://doi.org/10.14359/863>.
- Yang XY, Xie YM, Steven GP, Querin OM. Bidirectional evolutionary method for stiffness optimization. *AIAA J* 1999;37:1483–8.
- Habashneh M, Rad MM. Reliability based topology optimization of thermoelastic structures using bi-directional evolutionary structural optimization method. *Int J Mech Mater Des* 2023;1–16. <https://doi.org/10.1007/S10999-023-09641-0/FIGURES/7>.
- Shobeiri V. Topology optimization using bi-directional evolutionary structural optimization based on the element-free Galerkin method 2015;48:380–96. <https://doi.org/10.1080/0305215X.2015.1012076>. (<http://dx.doi.org/10.1080/0305215x20151012076>).
- Yang XY, Xie YM, Liu JS, Parks GT, Clarkson PJ. Perimeter control in the bidirectional evolutionary optimization method. *Struct Multidiscip Optim* 2003;24:430–40. <https://doi.org/10.1007/S00158-002-0256-5/METRICS>.
- Zhu Q, Han Q, Liu J. Topological optimization design on constrained layer damping treatment for vibration suppression of thin-walled structures via improved BESO method. *Aerosp Sci Technol* 2023;142:108600. <https://doi.org/10.1016/J.AST.2023.108600>.
- Shobeiri V. Bidirectional evolutionary structural optimization for nonlinear structures under dynamic loads. *Int J Numer Methods Eng* 2020;121:888–903. <https://doi.org/10.1002/NME.6249>.
- Zhou Y, Lin Q, Hong J, Yang N. Bidirectional evolutionary optimization design of material stiffness for the uniformity of the contact stress. *Eur J Mech - A/Solids* 2021;89:104288. <https://doi.org/10.1016/J.EURMECHSOL.2021.104288>.
- Dalkint A, Wallin M, Tortorelli DA. Structural stability and artificial buckling modes in topology optimization. *Struct Multidiscip Optim* 2021;64:1751–63. <https://doi.org/10.1007/S00158-021-03012-Z/FIGURES/10>.
- Gao X, Ma H. Topology optimization of continuum structures under buckling constraints. *Comput Struct* 2015;157:142–52. <https://doi.org/10.1016/J.COMPSTRUC.2015.05.020>.
- Kemmler R, Lipka A, Ramm E. Large deformations and stability in topology optimization. *Struct Multidiscip Optim* 2005;30:459–76. <https://doi.org/10.1007/S00158-005-0534-0/METRICS>.
- Rad MM. A review of elasto-plastic shakedown analysis with limited plastic deformations and displacements. *Period Polytech Civ Eng* 2018;62:812–7. <https://doi.org/10.3311/PPCL11696>.
- Bian X, Fang Z. Large-scale buckling-constrained topology optimization based on assembly-free finite element analysis. *Adv Mech Eng* 2017;9:1–12. [https://doi.org/10.1177/1687814017715422/ASSET/IMAGES/LARGE/10.1177\\_1687814017715422-FIG14.JPEG](https://doi.org/10.1177/1687814017715422/ASSET/IMAGES/LARGE/10.1177_1687814017715422-FIG14.JPEG).
- Lindgaard E, Lund E, Rasmussen K. Nonlinear buckling optimization of composite structures considering “worst” shape imperfections. *Int J Solids Struct* 2010;47:3186–202. <https://doi.org/10.1016/j.ijlsolstr.2010.07.020>.
- Browne PA, Budd C, Gould NIM, Kim HA, Scott JA. A fast method for binary programming using first-order derivatives, with application to topology optimization with buckling constraints. *Int J Numer Methods Eng* 2012;92:1026–43. <https://doi.org/10.1002/NME.4367>.
- Bochenek B, Tajs-Zielińska K. Minimal compliance topologies for maximal buckling load of columns. *Struct Multidiscip Optim* 2015;51:1149–57. <https://doi.org/10.1007/S00158-014-1202-Z/FIGURES/26>.
- Gao X, Li L, Ma H, Gao X, Li L, Ma H. An adaptive continuation method for topology optimization of continuum structures considering buckling constraints. *Int J Appl Mech* 2017;9:1750092. <https://doi.org/10.1142/S1758825117500922>. (<https://doi.org/10.1142/S1758825117500922>).
- Papaioannou I, Daub M, Drieschner M, Duddeck F, Ehre M, Eichner L, et al. Assessment and design of an engineering structure with polymorphic uncertainty quantification. *GAMM-Mitt* 2019;42:e201900009. <https://doi.org/10.1002/GAMM.201900009>.
- Drieschner M, Petryna Y, Eichner L. Design of a 3D composite structure considering data uncertainties and various failure mechanisms. *PAMM* 2021;21:e202100030. <https://doi.org/10.1002/PAMM.202100030>.
- Schmidt A, Lahmer T. Efficient domain decomposition based reliability analysis for polymorphic uncertain material parameters. *PAMM* 2021;21:e202100014. <https://doi.org/10.1002/PAMM.202100014>.
- Schietzold FN, Richter B, Graf W, Kaliske M. Optimization of glulam beams with spatially dependent polymorphic uncertainty modeling of structural inhomogeneity in virtual boards. *PAMM* 2023;22:e202100255. <https://doi.org/10.1002/PAMM.202100255>.
- Li Z, Wang L, Lv T. Additive manufacturing-oriented concurrent robust topology optimization considering size control. *Int J Mech Sci* 2023;250:108269. <https://doi.org/10.1016/J.IJMECSCI.2023.108269>.
- Edler P, Freitag S, Kremer K, Meschke G. Optimization approaches for the numerical design of structures under consideration of polymorphic uncertain data. *ASCE-ASME J Risk Uncertain Eng Syst, Part B: Mech Eng* 2019;5:41013.
- Li Z, Wang L, Gu K. Efficient reliability-based concurrent topology optimization method under PID-driven sequential decoupling framework. *Thin-Walled Struct* 2024;203:112117. <https://doi.org/10.1016/J.TWS.2024.112117>.
- Jalalpour M, Tootkaboni M. An efficient approach to reliability-based topology optimization for continua under material uncertainty. *Struct Multidiscip Optim* 2016;53:759–72. <https://doi.org/10.1007/S00158-015-1360-7/FIGURES/8>.
- Lógo J, Ghaemi M, Rad MM. Optimal topologies in case of probabilistic loading: the influence of load correlation. *Mech Based Des Struct Mach* 2009;37:327–48. <https://doi.org/10.1080/15397730902936328>.
- Kharmanda G, Olhoff N, Mohamed A, Lemaire M. Reliability-based topology optimization. *Struct Multidiscip Optim* 2004;26:295–307. <https://doi.org/10.1007/S00158-003-0322-7/METRICS>.
- Lógo J, Rad MM, Knabel J, Tauzowski P. Reliability based design of frames with limited residual strain energy capacity. *Period Polytech Civ Eng* 2011;55:13–20. <https://doi.org/10.3311/PP.CI.2011-1.02>.
- Habashneh M, Movahedi Rad M. Reliability based geometrically nonlinear bi-directional evolutionary structural optimization of elasto-plastic material. *Sci Rep* 2022;12:1–22. <https://doi.org/10.1038/s41598-022-09612-z>.
- Luo Y, Zhou M, Wang MY, Deng Z. Reliability based topology optimization for continuum structures with local failure constraints. *Comput Struct* 2014;143:73–84. <https://doi.org/10.1016/J.COMPSTRUC.2014.07.009>.
- Jung HS, Cho S. Reliability-based topology optimization of geometrically nonlinear structures with loading and material uncertainties. *Finite Elem Anal Des* 2004;41:311–31. <https://doi.org/10.1016/J.FINEL.2004.06.002>.
- Eom YS, Yoo KS, Park JY, Han SY. Reliability-based topology optimization using a standard response surface method for three-dimensional structures. *Struct Multidiscip Optim* 2011;43:287–95. <https://doi.org/10.1007/S00158-010-0569-8/FIGURES/8>.

- [36] Balogh B, Bruggi M, Lógó J. Optimal design accounting for uncertainty in loading amplitudes: a numerical investigation. *Mech Based Des Struct Mach* 2018;46: 552–66. <https://doi.org/10.1080/15397734.2017.1362987>.
- [37] Nishino T, Kato J. Robust topology optimization based on finite strain considering uncertain loading conditions. *Int J Numer Methods Eng* 2021;122:1427–55. <https://doi.org/10.1002/NME.6584>.
- [38] Bruggi M, Ismail H, Lógó J. Topology optimization with graded infill accounting for loading uncertainty. *Compos Struct* 2023;311:116807. <https://doi.org/10.1016/J.COMPSTRUCT.2023.116807>.
- [39] Lógó J. New type of optimality criteria method in case of probabilistic loading conditions. *Mech Based Des Struct Mach* 2007;35:147–62. <https://doi.org/10.1080/15397730701243066>.
- [40] Gao X, Chen W, Li Y, Chen G. Robust topology optimization of multi-material structures under load uncertainty using the alternating active-phase method. *Compos Struct* 2021;270:114065. <https://doi.org/10.1016/J.COMPSTRUCT.2021.114065>.
- [41] Movahedi Rad M, Habashneh M, Lógó J. Reliability based bi-directional evolutionary topology optimization of geometric and material nonlinear analysis with imperfections. *Comput Struct* 2023;287:107120. <https://doi.org/10.1016/J.COMPSTRUCT.2023.107120>.
- [42] Smith M. *ABAQUS/Standard User's Manual, Version 6.9*. United States: Dassault Systèmes Simulia Corp; 2009.
- [43] Koiter WT. *A translation of the stability of elastic equilibrium*. Management Information Services; 1970.
- [44] Liguori FS, Madeo A, Magisano D, Leonetti L, Garcea G. Post-buckling optimisation strategy of imperfection sensitive composite shells using Koiter method and Monte Carlo simulation. *Compos Struct* 2018;192:654–70. <https://doi.org/10.1016/J.COMPSTRUCT.2018.03.023>.
- [45] Deml M, Wunderlich W. Direct evaluation of the 'worst' imperfection shape in shell buckling. *Comput Methods Appl Mech Eng* 1997;149:201–22. [https://doi.org/10.1016/S0045-7825\(97\)00055-8](https://doi.org/10.1016/S0045-7825(97)00055-8).
- [46] Movahedi Rad M, Habashneh M, Lógó J. Elasto-Plastic limit analysis of reliability based geometrically nonlinear bi-directional evolutionary topology optimization. *Structures* 2021;34:1720–33. <https://doi.org/10.1016/j.istruc.2021.08.105>.
- [47] Yang XY, Xie YM, Liu JS, Parks GT, Clarkson PJ. Perimeter control in the bidirectional evolutionary optimization method. *Struct Multidiscip Optim* 2003; 24:430–40. <https://doi.org/10.1007/S00158-002-0256-5/METRICS>.
- [48] Querin OM, Young V, Steven GP, Xie YM. Computational efficiency and validation of bi-directional evolutionary structural optimisation. *Comput Methods Appl Mech Eng* 2000;189:559–73. [https://doi.org/10.1016/S0045-7825\(99\)00309-6](https://doi.org/10.1016/S0045-7825(99)00309-6).
- [49] Li Q, Steven GP, Xie YM. A simple checkerboard suppression algorithm for evolutionary structural optimization. *Struct Multidiscip Optim* 2001;22:230–9. <https://doi.org/10.1007/S001580100140/METRICS>.
- [50] Huang X, Xie M. *Evolutionary topology optimization of continuum structures: methods and applications*. John Wiley & Sons; 2010. <https://doi.org/10.1002/9780470689486>.
- [51] Huang X, Xie YM. Convergent and mesh-independent solutions for the bi-directional evolutionary structural optimization method. *Finite Elem Anal Des* 2007;43:1039–49. <https://doi.org/10.1016/j.finel.2007.06.006>.
- [52] Huang X, Xie YM, Burry MC. Advantages of bi-directional evolutionary structural optimization (BESO) over evolutionary structural optimization (ESO). *Adv Struct Eng* 2007;10:727–37. <https://doi.org/10.1260/136943307783571436>.
- [53] Wu J, Gao J, Luo Z, Brown T. Robust topology optimization for structures under interval uncertainty. *Adv Eng Softw* 2016;99:36–48. <https://doi.org/10.1016/J.ADVENGSOFT.2016.05.002>.
- [54] Liu J, Wen G, Qing Q, Xie YM. An efficient method for topology optimization of continuum structures in the presence of uncertainty in loading direction. *Int J Comput Methods* 2016;14. <https://doi.org/10.1142/S0219876217500542>. (<https://doi.org/10.1142/S0219876217500542>).
- [55] Choi SK, Canfield RA, Grandhi RV. Reliability-based structural design. *Reliability-Based Structural Design* 2007:1–306. <https://doi.org/10.1007/978-1-84628-445-8/COVER>.
- [56] Haldar A, Mahadevan S. *Probability, reliability, and statistical methods in engineering design*. John Wiley & Sons Incorporated; 2000.
- [57] Yun X, Wang Z, Gardner L. Full-range stress–strain curves for aluminum alloys. *J Struct Eng* 2021;147:4021060. [https://doi.org/10.1061/\(ASCE\)ST.1943-541X.0002999](https://doi.org/10.1061/(ASCE)ST.1943-541X.0002999).
- [58] Yun X, Wang Z, Gardner L. Full-range stress–strain curves for aluminum alloys. *J Struct Eng* 2021;147:4021060. [https://doi.org/10.1061/\(ASCE\)ST.1943-541X.0002999](https://doi.org/10.1061/(ASCE)ST.1943-541X.0002999).
- [59] Movahedi Rad M, Habashneh M, Lógó J. Elasto-plastic limit analysis of reliability based geometrically nonlinear bi-directional evolutionary topology optimization. *Structures* 2021;34:1720–33. <https://doi.org/10.1016/J.ISTRUC.2021.08.105>.